2013 European Control Conference (ECC)
July 17-19, 2013, Zürich, Switzerland.

Fractional Order Identification of Human Arm Dynamics: Preliminary Results*

Inés Tejado, Duarte Valério, Pedro Pires and Jorge Martins

Abstract— **Recently, control approaches for human-like behaviour have been attracting considerable attention in the field of surgery robotics. To this respect, precise dynamic models of the human arm are required to give the surgeon the physical feeling of working with a human assistant rather than a machine, which will result in a safer physical interaction. Musculo-skeletal systems of several species, including human muscles, have been successfully modelled by fractional differential equations. This study presents fractional order closed-loop identification for estimating the dynamics of the human arm. In particular, fractional and integer order models are identified in the frequency domain from real experiments with human subjects, using continuous random force as input and position in angle as output. The results show that more general dynamic models, i.e., fractional order models, allow adequate frequency responses to be attained but with a smaller number of parameters. A comparison with different dynamic models of the human arm reported in the literature is also given to demonstrate the validity of the proposed models.**

I. INTRODUCTION

When developing control architectures for surgery robotics, it is often necessary to use a model of the human operator. Controlling a robot to behave like a musculo-skeletal system lowers the dynamic discontinuity between the surgeon's arm and the robotic arm, which in turn gives the surgeon the physical feeling of working with a human assistant rather than a machine. Furthermore, this contributes to a safer physical interaction, to an increase in surgeon comfort and ergonomics, and at the outset wins over the traditional scepticism surgeons have to robotic intervention in the operating room. Refer e.g. to [19], [2], [12], [13] for remarkable opportunities offered by integrating human and robot into a single system.

In what concerns human arm models, and while they are in reality non-linear, time-varying systems, it is commonly accepted to consider third order integer dynamic models for comparison and validation purposes, in which the human arm was considered as a mechanical system consisting of five elements — one mass, two springs and two dampers [6], [4], [18], [3]. Other more complex models for the human arm were also proposed, applying different methods for the identification (see e.g. [1], [10], [9], [24]).

*Inés Tejado would like to thank the Portuguese Fundação para a Ciência e a Tecnologia (FCT) for the grant with reference SFRH/BPD/81106/2011. This work was also supported by national funding through FCT, under project Pest/OE/EME/LA0022/2011 — LAETA/IDMEC/CSI.

I. Tejado, D. Valério, P. Pires and J. Martins are with LAETA/IDMEC, Instituto Superior Técnico, Universidade Técnica de Lisboa, 1049-001 Lisbon, Portugal. email: {ines.tejado;duarte.valerio}@ist.utl.pt, {pedropires;jorgemartins}@ist.utl.pt

Some recent works highlight a fractal structure of muscles, which often leads to fractional dynamics; this alone justifies the approach based on the use of a non integer (or fractal) model to characterise its dynamic behaviour. A fractional structure model, due to its infinite dimension nature, is particularly adapted to model complex systems with few parameters and to obtain an adequate exploitable model [7]. To this respect, muscles of several species, including human muscles, have been successfully modelled by fractional differential equations (see e.g. [17], [16], [15], [5]). However, up to now fractional identification methods have not been applied to human arm dynamics.

Given this motivation, the aim of this paper is twofold:

1) Measure, record and characterise the dynamic of the human arm under muscle co-contraction by extending the method performed in [6] to fractional order models, with the measured force at the hand as model input and the measured elbow angle —instead of the position— as output.
2) Offer a comparative study with current models reported in the literature.

It is worth remarking that it is the first step to achieve the final objective of this work, viz., to control the position of the end of a surgery robot.

The remainder of this paper is organised as follows. Section II summarizes the fractional order identification method used in this work, Levy's method. Section III describes the experiments and processing performed to estimate the frequency response of the human arm. In Section IV, the dynamic arm models identified are presented, including a comparison with other models reported in the literature. Finally, Section V draws the conclusions of this paper.

II. FRACTIONAL ORDER IDENTIFICATION

The identification of a fractional model directly from a time response is reviewed in [8]; a survey of methods for both time and frequency responses can be found in [22].

In this paper, as explained below in detail in section III-B, a frequency response was obtained first, and models were then identified using Levy's method. This method fits, to a frequency response $G(j\omega_p),\ p = 1, \ldots, f$, a commensurable fractional model of order α with frequency response given by

$$\hat{G}(j\omega_p) = \frac{\sum_{k=0}^{m} b_k (j\omega_p)^{k\alpha}}{1 + \sum_{k=1}^{n} a_k (j\omega_p)^{k\alpha}} = \frac{N(j\omega_p)}{D(j\omega_p)}. \qquad (1)$$

Notice that, without loss of generality, we have made $a_0 = 1$. The adjustment might be done minimising

$\left|G(j\omega) - \frac{N(j\omega)}{D(j\omega)}\right|^2$, but it is easier to minimise instead

$$\begin{aligned}|E|^2 &= (GD - N)^2 = \\ &= \Big[\Big(\Re[G] + j\Im[G]\Big)\Big(\Re[D] + j\Im[D]\Big) \\ &\quad - \Big(\Re[N] + j\Im[N]\Big)\Big]^2 \\ &= \Big[\Big(\Re[G]\Re[D] - \Im[G]\Im[D] - \Re[N]\Big) \\ &\quad + j\Big(\Re[G]\Im[D] + \Im[G]\Re[D] - \Im[N]\Big)\Big]^2 \\ &= \Big(\Re[G]\Re[D] - \Im[G]\Im[D] - \Re[N]\Big)^2 \\ &\quad + \Big(\Re[G]\Im[D] + \Im[G]\Re[D] - \Im[N]\Big)^2, \end{aligned} \tag{2}$$

where $\Re[-]$ and $\Im[-]$ denote real and imaginary parts, respectively. $|E|^2$ is then differentiated with respect to coefficients $b_i,\ i = 0, 1, \ldots, m$ and $a_i,\ i = 1, 2, \ldots, n$, and the derivative is equalled to zero. This is done for all frequencies, resulting in a system of equations given by

$$\begin{bmatrix} \mathbf{A} & \mathbf{B} \\ \mathbf{C} & \mathbf{D} \end{bmatrix} \begin{bmatrix} \mathbf{b} \\ \mathbf{a} \end{bmatrix} = \begin{bmatrix} \mathbf{e} \\ \mathbf{g} \end{bmatrix} \tag{3}$$

$$\mathbf{A} = \sum_{p=1}^{f} {}_p\mathbf{A} \tag{4}$$

$${}_p\mathbf{A}_{l,c} = -\Re\left[(j\omega_p)^{l\alpha}\right]\Re\left[(j\omega_p)^{c\alpha}\right] - \Im\left[(j\omega_p)^{l\alpha}\right]\Im\left[(j\omega)^{c\alpha}\right], \quad l = 0\ldots m \wedge c = 0\ldots m \tag{5}$$

$$\mathbf{B} = \sum_{p=1}^{f} {}_p\mathbf{B} \tag{6}$$

$$\begin{aligned}{}_p\mathbf{B}_{l,c} &= \Re\left[(j\omega_p)^{l\alpha}\right]\Re\left[(j\omega)^{c\alpha}\right]\Re\left[G(j\omega_p)\right] \\ &\quad + \Im\left[(j\omega_p)^{l\alpha}\right]\Re\left[(j\omega_p)^{c\alpha}\right]\Im\left[G(j\omega_p)\right] \\ &\quad - \Re\left[(j\omega_p)^{l\alpha}\right]\Im\left[(j\omega)^{c\alpha}\right]\Im\left[G(j\omega)\right] \\ &\quad + \Im\left[(j\omega_p)^{l\alpha}\right]\Im\left[(j\omega_p)^{c\alpha}\right]\Re\left[G(j\omega_p)\right], \\ &\quad l = 0\ldots m \wedge c = 1\ldots n \end{aligned} \tag{7}$$

$$\mathbf{C} = \sum_{p=1}^{f} {}_p\mathbf{C} \tag{8}$$

$$\begin{aligned}{}_p\mathbf{C}_{l,c} &= -\Re\left[(j\omega_p)^{l\alpha}\right]\Re\left[(j\omega)^{c\alpha}\right]\Re\left[G(j\omega_p)\right] \\ &\quad + \Im\left[(j\omega_p)^{l\alpha}\right]\Re\left[(j\omega_p)^{c\alpha}\right]\Im\left[G(j\omega_p)\right] \\ &\quad - \Re\left[(j\omega_p)^{l\alpha}\right]\Im\left[(j\omega)^{c\alpha}\right]\Im\left[G(j\omega_p)\right] \\ &\quad - \Im\left[(j\omega_p)^{l\alpha}\right]\Im\left[(j\omega_p)^{c\alpha}\right]\Re\left[G(j\omega_p)\right], \\ &\quad l = 1\ldots n \wedge c = 0\ldots m \end{aligned} \tag{9}$$

$$\mathbf{D} = \sum_{p=1}^{f} {}_p\mathbf{D} \tag{10}$$

$$\begin{aligned}{}_p\mathbf{D}_{l,c} &= \left(\Re\left[G(j\omega_p)\right]^2 + \Im\left[G(j\omega_p)\right]^2\right) \\ &\quad \left(\Re\left[(j\omega_p)^{l\alpha}\right]\Re\left[(j\omega_p)^{c\alpha}\right] + \Im\left[(j\omega_p)^{l\alpha}\right]\Im\left[(j\omega_p)^{c\alpha}\right]\right), \\ &\quad l = 1\ldots n \wedge c = 1\ldots n \end{aligned} \tag{11}$$

$$\mathbf{e} = \sum_{p=1}^{f} {}_p\mathbf{e} \tag{12}$$

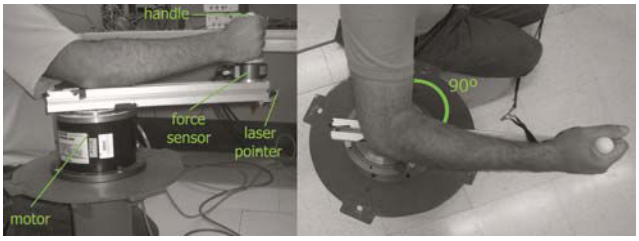

Fig. 1. Experimental set-up used for collecting experimental data of human arm dynamics: frontal view (left) and top view (right)

$${}_p\mathbf{e}_{l,1} = -\Re\left[(j\omega_p)^{l\alpha}\right]\Re\left[G(j\omega_p)\right] - \Im\left[(j\omega_p)^{l\alpha}\right]\Im\left[G(j\omega_p)\right], \quad l = 0\ldots m \tag{13}$$

$$\mathbf{g} = \sum_{p=1}^{f} {}_p\mathbf{g} \tag{14}$$

$${}_p\mathbf{g}_{l,1} = -\Re\left[(j\omega_p)^{l\alpha}\right]\left(\Re\left[G(j\omega_p)\right]^2 + \Im\left[G(j\omega_p)\right]^2\right), \quad l = 1\ldots n \tag{15}$$

$$\mathbf{b} = [b_0 \cdots b_m]^T \tag{16}$$

$$\mathbf{a} = [a_1 \cdots a_n]^T \tag{17}$$

If the appropriate order α is not known, and since including it explicitly among the parameters to minimise would lead to a nonlinear problem, it is expedient to find models for several different values of α and keep the best [22]. For alternative formulations and possible improvements of this identification method, see [21], [22].

III. METHODS

This section addresses the two-stage method proposed in this preliminary study to identify the dynamics of the human arm. Firstly, details of the subjects, equipments and trials are given and, then, the subsequent data processing to estimate the frequency response of the arm is explained.

A. Description of the experiments

Up to now, two healthy males without any known musculo-skeletal injuries of the higher limbs volunteered to participate in this study with prior consent, using their right arm.

Experiments were performed using a Kollmorgen direct drive motor D061M-23-1310 model in current control mode, which was able to produce 5.3 Nm continuous torque and 16.9 Nm peak torque. For safety reasons, the motor rotation angle had a limited range of action of 0.9 rad in both directions around the zero-point. The motor current was controlled using an advanced Kollmorgen drives (AKD) controller with a 16-bit analog input used for the current reference input and an encoder output emulator for the measured angle. An aluminium horizontal link was attached to the rotatory center of the motor, with a handle and a laser pointer mounted at its end. The laser was used to point the position of the arm-link group on a screen which was in front of the motor; at the beginning of each trial, the pointer was aligned with the zero position marked in the screen. To measure forces applied by

the subjects in the Y axis, a JR3 12-degree-of-freedom DSP-based force sensor, connected to a PCI-BUS dual receiver board, was placed at the handle aligned accordingly with the scheme in Fig. 3. The JR3 measured linear forces and moments along with linear and angular accelerations. Its output was a 16-bit digital signal that could be associated with a digital filter directly implemented into the JR3 DSP sensor. For data acquisition, an Intel I7 computer with XPC-Target operating system running at 2 kHz frequency was used. This target computer had a MF624 Humusoft analog-digital PCI board for digital-analog communications and a JR3 PCI-BUS dual receiver board.

Let us consider the motor–link–sensor dynamics as follows:

$$M\ddot{\theta} + C(\dot{\theta}, \theta) = \tau, \tag{18}$$

where M and C are the mass matrix and the friction term dynamics, respectively, and the applied torque τ is

$$\tau = K_{Torque} I_C, \tag{19}$$

being K_{Torque} and I_C the motor torque constant and current input, respectively. In (18), it is desirable to eliminate all the motor-link-sensor dynamics in order to be able to measure only the human arm dynamics. To this end, the applied motor torque was

$$\tau = \tau_{Dyn} + \tau_{External}, \tag{20}$$

in which τ_{Dyn} refers to a dynamic compensation given by

$$\tau_{Dyn} = \hat{M}\ddot{\theta} + F = \hat{M}\ddot{\theta} + \hat{C}\dot{\theta} + \hat{B}\ sign(\dot{\theta}), \tag{21}$$

where $\hat{M}$ is the estimated mass matrix and F, the friction model. It is worth remarking that compensation (21) is as good as the estimation of $\hat{M}$ and F. For this experiment, a simple Coulomb friction model revealed sufficient, since the motor in question is a direct drive motor without the drawbacks of gear backlash. Moreover, to increase the force control robustness, a PID controller was added as presented in the block scheme in Fig. 3. In fact, this control implementation guaranteed sufficient bandwidth to capture all the dynamic properties of the human arm.

During each experiment, subjects were kneeling on one side of the motor, grabbing the handle with an angle for the elbow of about 90° as shown in Fig. 1. Although the elbow and wrists were not supported, they were asked not only to maintain a firm grip on the handle but also not to move their trunk, shoulder and elbow. Likewise, during each trial the subjects were required to keep the laser pointer at zero-point under muscle co-contraction.

In order to avoid subject fatigue, the duration of each trial was 40 s. Human anticipatory reflexes make modelling the arm dynamics difficult, as it is hard to keep the arm passive to force disturbances. Fortunately, the more random the force disturbance is, the less likely it will trigger the arm's reflexes [6]. For this reason, the current study used inputs generated by a sum of sinusoids with frequencies in the $[0.12, 15]$ Hz range, and limited to not exceed 5 N, to render them unpredictable by the subjects under experiment and allow us to obtain frequency responses in the mentioned range.

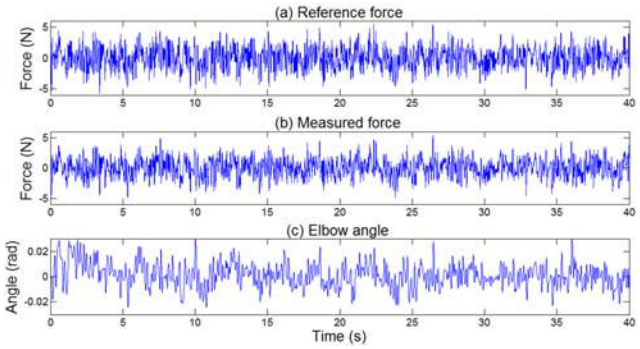

Fig. 2. Example of signals involved in one experiment: (a) Reference force (b) Measured force (c) Elbow angle

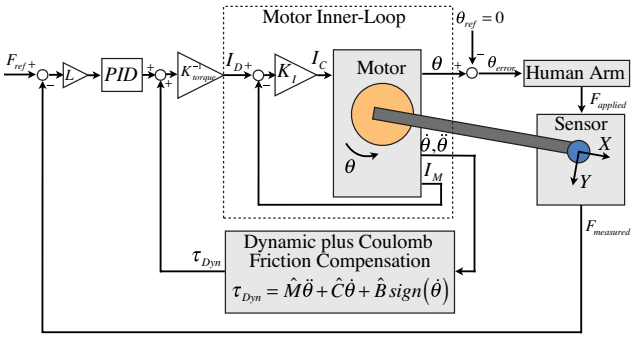

Fig. 3. Closed-loop block scheme for identification of human arm dynamics. F_{ref}, $F_{applied}$ and $F_{measured}$ are the input, applied (by the subject) and measured (by the sensor) forces, respectively (indeed, it is assumed that $F_{applied} = F_{measured}$); θ_{ref}, θ and θ_{error} are the reference, measured and error angles, respectively ($\theta_{ref} = 0$, i.e., subjects are required to maintain the link at zero-point); L is the link length (for this experiment, $L = 0.35$ m); K_I and K_{torque} are the motor current control gain and torque constant, respectively; and I_D, I_M and I_C are the reference, measured and applied currents of the motor, respectively

Fig. 2 shows an example of signals involved in one of the experiments. The force measured by the mentioned sensor was practically identical to the force input. It was assumed that the bandwidth for the human arm is approximated to 10 Hz, fact which justifies the selection of 15 Hz bandwidth for the force input.

Both the force applied by the subject, $F_{applied}(t)$, and the elbow angle, $\theta(t)$, were recorded with a sampling frequency of 2 kHz. Fig. 3 shows a block scheme of the experimental set-up, with which the desired dynamic human arm transfer function was determined as

$$G_{arm}(s) = \frac{\theta(s)}{F_{measured}(s)}. \tag{22}$$

B. Data processing

In order to identify the dynamics of the human arm from our experiments by Levy's method, the estimation of the corresponding frequency response is needed. To do so, an approach for estimating transfer functions of linear systems from spectral analysis will be used. Spectral estimation was applied to human arm modelling in [6], [11], [23]. In

particular, the measured human experiment frequency response is computed by using Welch's method —by means of the MATLAB function *tfestimate*— with 18 Blackmanharris-windowed segments (length of the window equal to 5000), 18000 samples and 25% overlap in order to attain smooth frequency responses. Previously, the output was filtered by a zero-phase forward and reverse FIR equal ripple digital filter —applied with MATLAB function *filtfilt*— designed with pass-band and stop-band frequencies of 15 Hz and 18 Hz, respectively, and a passband ripple of 1 dB with 80 dB of stop-band attenuation.

It should be noticed that the variations of Levy's method mentioned at the end of section II — the use of weights to correct an excessive influence of high-frequency data [25], [22], or the use of iterations to minimise $\left|G-\frac{N}{D}\right|^2$ rather than $|GD-N|^2$ [22], [14] — have been attempted, without improvement in results.

IV. RESULTS

In this section, the dynamic models for the human arm resulting of the identification are presented and also compared with the other models reported in the literature.

A. Dynamic models

Let us consider a general model, corresponding to frequency response (1); its (fractional) transfer function of commensurable order α as follows:

$$\hat{G}(s)=\frac{\sum_{k=0}^{m} b_k s^{k\alpha}}{1+\sum_{k=1}^{n} a_k s^{k\alpha}}. \tag{23}$$

Each model was identified to accurately reflect the mean value of the measured frequency responses in the $[0.12, 15]$ Hz range by means of Levy's method in Matlab (with *levy* function [20]) for fractional and integer order models up to third order in accordance with [6]. Commensurable orders of fractional models were found sweeping the $\alpha \in]0,2[$ range, where models are stable, with a 0.1 step, and keeping the best result. In order to evaluate the goodness-of-fit of the obtained models, the following performance indices were calculated:

1) Mean square error (MSE) per sampling frequency, defined as

$$MSE=\frac{\sum_{j=1}^{N}(g_j-\hat{g}_j)^2}{N}, \tag{24}$$

where g_j and $\hat{g}_j$ are the experimental and estimated frequency responses, respectively, and N is the number of frequency samples.

2) Mean absolute deviation (MAD) as

$$MAD=\frac{\sum_{j=1}^{N}|g_j-\hat{g}_j|}{N}. \tag{25}$$

3) Coefficient of determination ($R^2 \in (0,1)$) defined as

$$R^2=1-\frac{\sum_{j=1}^{N}(g_j-\hat{g}_j)^2}{\sum_{j=1}^{N}(g_j-\bar{g})^2}, \tag{26}$$

where $\bar{g}$ is the mean of the experimental response. This parameter gives an idea of how successful the fit is in explaining the variation of the data: the closer to 1, the better the fit.

The best results were obtained for the following fractional and integer order models:

$$\begin{aligned}\hat{G}_{IO}(s)&=\frac{b_2s^2+b_1s+b_0}{a_3s^3+a_2s^2+a_1s+1}= \\ &=\frac{5.32{\cdot}10^{-7}s^2+1.86{\cdot}10^{-5}s+0.005}{8.75{\cdot}10^{-6}s^3+7.81{\cdot}10^{-4}s^2+0.034s+1},\end{aligned} \tag{27}$$

$$\begin{aligned}\hat{G}_{FO,I}(s)&=\frac{b_1s^{\alpha_1}+b_0}{a_2s^{2\alpha_1}+a_1s^{\alpha_1}+1}= \\ &=\frac{6.375{\cdot}10^{-6}s^{1.4}+0.0037}{3.121{\cdot}10^{-5}s^{2.8}+0.0103s^{1.4}+1},\end{aligned} \tag{28}$$

$$\begin{aligned}\hat{G}_{FO,II}(s)&=\frac{b_0}{a_2s^{2\alpha_2}+a_1s^{\alpha_2}+1}= \\ &=\frac{0.0035}{3.296{\cdot}10^{-4}s^{2.2}+0.0184s^{1.1}+1}.\end{aligned} \tag{29}$$

Two of the identified models were of fractional order, with an order less than 3, whereas the integer model was of third order. At this point, it is important to remark that these models have a similar structure that the widely used in the literature [6], which justifies the work developed up to now.

A comparison of the frequency responses of the identified models is illustrated in Fig. 4. It can be seen that the proposed arm models produce frequency responses that closely match the experimental ones, especially in $[3, 15]$ Hz range (for high frequencies). This fact may suggest the need for further study at low frequencies. Likewise, Fig. 5 shows their time responses. It can be seen that all models adequately follow the input —the measured force in this case—, but the integer model (27) seems to have often oscillations with a too high amplitude. Note that the experimental angle represented in this figure was obtained as the mean of the collected from both examining subjects.

A summary of the identification results is given in Table I. From them, it can be stated that only slight differences can be found between the obtained models in terms of the performance indices, particularly for models (27) and (28). On the contrary, the main and significant difference arises from the number of parameters necessary to determine the model. Actually, it is shown that fractional order models allow adequate frequency responses to be attained, but with less parameters; while integer models, with less parameters, have unacceptable performances. To this respect, additional integer order models with 3 and 4 parameters were also included in Table I —referred to as model A (two poles) and B (two poles and one zero), respectively—. Due to this fact, henceforth we considered the dynamics of the human arm given by the following transfer function:

$$\hat{G}_{arm}(s)=\frac{6.375{\cdot}10^{-6}s^{1.4}+0.0037}{3.121{\cdot}10^{-5}s^{2.8}+0.0103s^{1.4}+1}. \tag{30}$$

B. Comparison with other studies

As mentioned previously, several papers focused on the identification of the human arm dynamics in the frequency

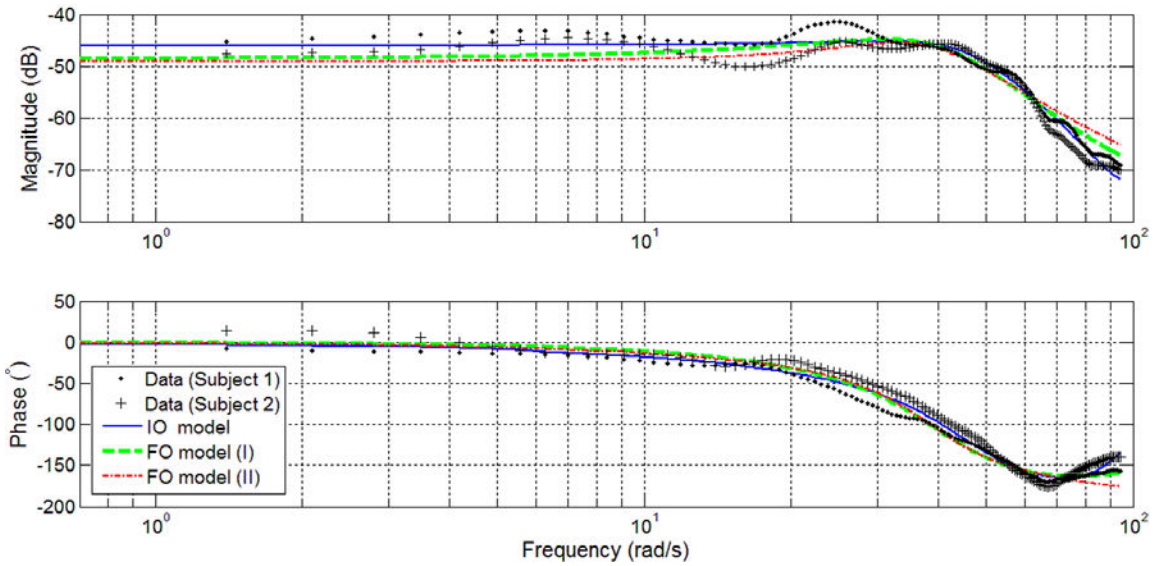

Fig. 4. Frequency responses of the identified fractional order (FO) models (28) and (29) and the integer order (IO) model (27). The dotted lines correspond to the experimental responses of the human arm

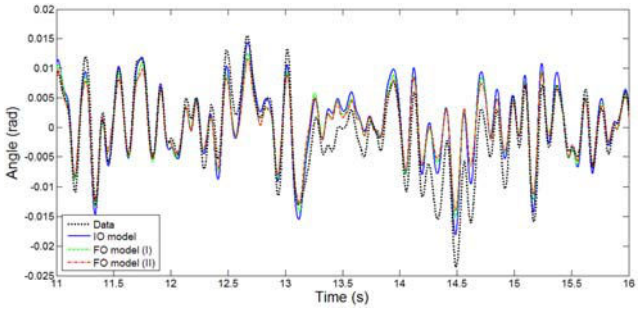

Fig. 5. Time responses of the identified fractional order (FO) models (28) and (29) and the integer order (IO) model (27) (11−16 s of the experiment). The dotted line corresponds to the mean of the elbow angles measured for Subject 1 and 2

TABLE I

SUMMARY OF THE IDENTIFICATION RESULTS

Model	α	MSE ($\times 10^{-7}$)	MAD ($\times 10^{-4}$)	R^2	# param
(27)	1	2.70	3.52	0.94	5
(28)	1.4	5.14	5.01	0.89	4
(29)	1.1	8.4	6.37	0.82	3
A	1	11.52	6.71	0.8	3
B	1	11.59	6.72	0.8	4

domain assume that the human arm can be conceptualized as a mechanical model consisting of five elements: one mass (M), which represents the inertia of the arm, two springs (with constants k_1 and k_2) and two dampers (with damping coefficients d_1 and d_2), where each damper-spring group represents the hand grasp and the arm stiffness (see [6] and references therein for a recent review). Thus, the transfer functions of these models were expressed as

$$\hat{G}_{arm}(s) = \frac{b_2 s^2 + b_1 s + b_0}{a_3 s^3 + a_2 s^2 + a_1 s + 1}, \tag{31}$$

where

$$b_2 = M/(k_1 k_2), \tag{32}$$
$$b_1 = (d_1 + d_2)/(k_1 k_2), \tag{33}$$
$$b_0 = (k_1 + k_2)/(k_1 k_2), \tag{34}$$
$$a_3 = d_1 M/(k_1 k_2), \tag{35}$$
$$a_2 = (d_1 d_2 + k_1 M)/(k_1 k_2), \tag{36}$$
$$a_1 = (k_1 d_2 + k_2 d_1)/(k_1 k_2). \tag{37}$$

Fig. 6 compares the frequency responses of different reported models with the one proposed in this study; their parameters and an estimation of their bandwidth —denoted as BW—, measured at the frequency where gain is -3 dB, can be found in Table II. Although the experimental methods differ significantly, it is important to highlight that the structure of all models is comparable. As can be seen, the estimated BW of our model differs from all others because of the different configuration, discussed in section III-A. Notice that of all models ours is the one with a smaller number of parameters to determine.

V. CONCLUSION

This study has presented integer and fractional order models for the human arm dynamics obtained from real experiments in the frequency domain. The structures of these models agree with results in the specialized literature. However, it was shown that fractional order models may allow adequate frequency responses to be attained but with less number of parameters.

The importance of this preliminary work is not only to have measured, recorded and characterized the dynamic of

TABLE II

ARM MODELS FROM THE LITERATURE

	Parameters for model (31)							BW
	a_3 $(\times 10^{-7})$	a_2 $(\times 10^{-5})$	a_1 $(\times 10^{-2})$	b_2 $(\times 10^{-7})$	b_1 $(\times 10^{-6})$	b_0 $(\times 10^{-3})$	α	(Hz)
Diaz [4]	7.19	225.4	7.01	6.093	22.32	10.42	1	3.11
Speich [18]	2724	670.9	14.48	211	640.8	11.23	1	2.79
Vlugt [3]	304.4	316.9	6.28	1.71	19.58	1.431	1	3.83
Fu [6]	7.57	81.82	6.748	9.757	90.05	4.979	1	2.80
Tejado (30)	–	3.121	1.032	–	6.375	3.751	1.4	8.27

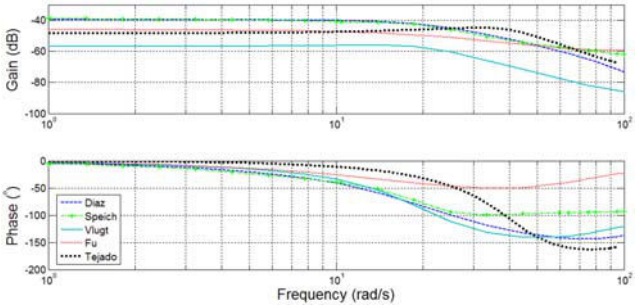

Fig. 6. Comparison of the frequency responses of different dynamic models of the human arm reported in the literature —Diaz [4], Speich [18], Vlugt [3] and Fu [6]— and the one obtained in the current study (black dotted line)

the human arm under co-contraction, obtaining similar results reported in the literature, but also to have extended the analysis to more general models, i.e., fractional order models.

Our future efforts will focus on the validation of the current models with the experimental data of more subjects and to design a proper controller for the surgery robot.

REFERENCES

[1] S. Adewusi, S. Rakheja, and P. Marcotte. Biomechanical models of the human hand-arm to simulate distributed biodynamic responses for different postures. *International Journal of Industrial Ergonomics*, 42(2):249–260, 2012.

[2] Yoseph Bar-Cohen. Humanlike robots: the upcoming revolution in robotics. *Proceedings of the SPIE*, 7401:740102, 2009.

[3] Erwin de Vlugt, Alfred C. Schouten, and Frans C.T. van der Helm. Adaptation of reflexive feedback during arm posture to different environments. *Biological Cybernetics*, 87(1):10–26, 2002.

[4] I. Diaz and J.J. Gil. Influence of vibration modes and human operator on the stability of haptic rendering. *IEEE Transactions on Robotics*, 26(1):160–165, 2010.

[5] Vladan D. Djordjevic, Jovo Jaric, Ben Fabry, Jeffrey J. Fredberg, and Dimitrije Stamenovic. Fractional derivatives embody essential features of cell rheological behavior. *Annals of Biomedical Engineering*, 31:692–699, 2003.

[6] M. J. Fu and M. C. Cavusoglu. Human-arm-and-hand-dynamic model with variability analyses for a stylus-based haptic interface. *IEEE Transactions on Systems, Man, and Cybernetics, Part B: Cybernetics*, PP(99):1–12, 2012.

[7] Richard L. Magin. *Fractional Calculus in Bioengineering*. Begell House, 2004.

[8] Rachid Malti, Stephane Victor, and Alain Oustaloup. Advances in system identification using fractional models. *ASME Journal of Computational and Nonlinear Dynamics*, 3:021401, 2008.

[9] F. Mobasser and K. Hashtrudi-Zaad. A method for online estimation of human arm dynamics. In *Proceedings of th 28th Annual International Conference of the IEEE Engineering in Medicine and Biology Society (EMBS'06)*, pages 2412–2416, 2006.

[10] H.J. Nagarsheth, P.V. Savsani, and M.A. Patel. Modeling and dynamics of human arm. In *Proceedings of the 2008 IEEE International Conference on Automation Science and Engineering (CASE'08)*, pages 924–928, 2008.

[11] J.J. Palazzolo, M. Ferraro, H.I. Krebs, D. Lynch, B.T. Volpe, and N. Hogan. Stochastic estimation of arm mechanical impedance during robotic stroke rehabilitation. *IEEE Transactions on Neural Systems and Rehabilitation Engineering*, 15(1):94–103, 2007.

[12] Shinsuk Park, Hokjin Lim, Byeong-sang Kim, and Jae-bok Song. Development of safe mechanism for surgical robots using equilibrium point control method. In Rasmus Larsen, Mads Nielsen, and Jon Sporring, editors, *Medical Image Computing and Computer-Assisted Intervention MICCAI 2006*, volume 4190 of *Lecture Notes in Computer Science*, pages 570–577. Springer Berlin / Heidelberg, 2006.

[13] Veljko Potkonjak, Spyros Tzafestas, Dragan Kostic, and Goran Djordjevic. Human-like behavior of robot arms: general considerations and the handwriting task - Part I: mathematical description of human-like motion: distributed positioning and virtual fatigue. *Robotics and Computer-Integrated Manufacturing*, 17(4):305–315, 2001.

[14] C. K. Sanathanan and J. Koerner. Transfer function synthesis as a ratio of two complex polynomials. *IEEE Transactions on Automatic Control*, 8:56–58, 1963.

[15] Laurent Sommacal, Pierre Melchior, Jean-Marie Cabelguen, Alain Oustaloup, and Auke Jan Ijspeert. *Advances in Fractional Calculus: Theoretical Developments and Applications in Physics and Engineering*, chapter Fractional Multimodels of the Gastrocnemius Muscle for Tetanus Pattern, pages 271–285. Springer, 2007.

[16] Laurent Sommacal, Pierre Melchior, Arnaud Dossat, Julied Petit, Jean-Marie Cabelguen, Alain Oustaloup, and Auke Jan Ijspeert. Improvement of the muscle fractional multimodel for low-rate stimulation. *Biomedical Signal Processing and Control*, 2:226–233, 2007.

[17] Laurent Sommacal, Pierre Melchior, Alain Oustaloup, Jean-Marie Cabelguen, and Auke Jan Ijspeert. Fractional multi-models of the frog gastrocnemius muscle. *Journal of Vibration and Control*, 14(9-10):1415–1430, 2008.

[18] John E. Speich, Liang Shao, and Michael Goldfarb. Modeling the human hand as it interacts with a telemanipulation system. *Mechatronics*, 15(9):1127–1142, 2005.

[19] Michel Taïx, Minh Tuan Tran, Philippe Sou ares, and Emmanuel Guigon. Generating human-like reaching movements with a humanoid robot: A computational approach. *Journal of Computational Science*, -(0):–, 2012.

[20] Duarte Valério. Toolbox ninteger for MatLab. Technical report, Technical University of Lisbon, 2005.

[21] Duarte Valério, Manuel Duarte Ortigueira, and José Sá da Costa. Identifying a transfer function from a frequency response. *ASME Journal of Computational and Nonlinear Dynamics*, 3(2):021207, 2008.

[22] Duarte Valério and José Sá da Costa. *An Introduction to Fractional Control*. IET, 2012. In print. ISBN 978-1-84919-545-4.

[23] Frans C.T. van der Helm, Alfred C. Schouten, Erwin de Vlugt, and Guido G. Brouwn. Identification of intrinsic and reflexive components of human arm dynamics during postural control. *Journal of Neuroscience Methods*, 119(1):1–14, 2002.

[24] G. Venture, K. Yamane, and Y. Nakamura. Identification of human musculo-tendon subject specific dynamics using musculo-skeletal computations and non linear least square. In *Proceedings of the 1st IEEE/RAS-EMBS International Conference onBiomedical Robotics and Biomechatronics (BioRob'06)*, pages 211–216, 2006.

[25] Blas Vinagre. *Modelado y control de sistemas dinámicos caracterizados por ecuaciones íntegro-diferenciales de orden fraccional*. PhD thesis, Universidad Nacional de Educación a Distancia, Madrid, 2001.